Biochemical and Biophysical Research Communications 431 (2013) 2–7

Contents lists available at SciVerse ScienceDirect

Biochemical and Biophysical Research Communications

journal homepage: www.elsevier.com/locate/ybbrc

Structure-based computational study of the hydrolysis of New Delhi metallo-β-lactmase-1

Kongkai Zhu [a,b,1], Junyan Lu [b,1], Fei Ye [b], Lu Jin [b], Xiangqian Kong [b], Zhongjie Liang [c], Yong Chen [a,*], Kunqian Yu [b], Hualiang Jiang [b], Jun-Qian Li [a], Cheng Luo [b,c,*]

[a] Department of Chemistry, Fuzhou University, Fujian 350108, China
[b] State Key Laboratory of Drug Research, Shanghai Institute of Materia Medica, Chinese Academy of Sciences, 555 Zuchongzhi Road, Shanghai 201203, China
[c] Center for Systems Biology, Soochow University, Jiangsu 215006, China

ARTICLE INFO

Article history:
Received 13 December 2012
Available online 9 January 2013

Keywords:
New Delhi metallo-β-lactmase-1
Metallo-β-lactamase
Molecular dynamics simulations
Molecular mechanics/Poisson–Boltzmann surface area

ABSTRACT

New Delhi metallo-β-lactmase-1 (NDM-1) is an enzyme that confers antibiotic resistance to bacteria and is thus a serious threat to human health. Almost all clinically available β-lactam antibiotics can be hydrolyzed by NDM-1. To determine the mechanism behind the wide substrate diversity and strong catalytic ability of NDM-1, we explored the molecular interactions between NDM-1 and different β-lactam antibiotics using computational methods. Molecular dynamics simulations and binding free energy calculations were performed on enzyme-substrate (ES) complex models of NDM-1-Meropenem, NDM-1-Nitrocefin, and NDM-1-Ampicillin constructed by molecular docking. Our computational results suggest that mutant residues Ile35 and Lys216, and active site loop L1 residues 65–73 in NDM-1 play crucial roles in substrate recognition and binding. The results of our study provide new insights into the mechanism behind the enhanced substrate binding and wider substrate spectrum of NDM-1 compared with its homologous enzymes CcrA and IMP-1. These insights may be useful in the discovery and design of specific and potent inhibitors against NDM-1.

1. Introduction

β-Lactam antibiotics, which inhibit enzymes that participate in bacterial cell wall synthesis, have long been the mainstay drugs for treating serious bacterial infections [1]. However, bacteria have developed several resistance mechanisms against β-lactam antibiotics. Among them, generation of β-lactamases, which hydrolyze the amide bond in β-lactam rings to inactivate β-lactam antibiotics, is an especially effective resistance mechanism developed by bacteria [2]. β-Lactamases can be grouped into four classes according to their sequence homology [3]. Class A, C, and D enzymes, generally called serine-β-lactamases, use a serine residue in the active site to hydrolyze β-lactam antibiotics. Class B enzymes, also called metallo-β-lactamases (MBLs), are characterized by the one or two zinc (Zn) ions that are indispensable for enzyme activity [4]. MBLs are of great concern from a public health standpoint because of their extensive dissemination all over the world. Genes that encode MBLs are usually located in several highly transmissible plasmids [5]. MBLs are capable of hydrolyzing almost all β-lactam antibiotics, including the "last resort" carbapenems [6]. To date, no MBLs inhibitors useful for clinical treatment have been identified [7].

New Delhi metallo-β-lactamase (NDM-1), a new member of MBLs, was first identified in a Swedish patient hospitalized in New Delhi, India [8]. Shortly after its discovery, NDM-1 spread to many countries worldwide [9]. The unprecedented spread and speed of dissemination of NDM-1 positive strains as well as their ability to confer resistance to almost all clinically used β-lactam antibiotics, pose serious threats to human health [10]. Almost all commercially available serine β-lactamase inhibitors have failed to inhibit NDM-1. Thus, the risk of NDM-1 co-harboring multiple and unstable resistance determinants and the resulting decrease in efficacy of treatment with antibacterial drugs are of serious concern to clinicians and scientists worldwide.

Despite the clinical significance of NDM-1, the dynamic characteristics of its interactions with different substrates have not been studied. In the present study, molecular interactions between NDM-1 and β-lactam antibiotics (Fig. S1) were studied using a combination of computational methods, including molecular dynamics (MD) simulation, Poisson–Boltzmann model and solvent accessibility (MM-PBSA) binding free energy calculation, and computational alanine scanning. The results showed that NDM-1 binds to nitrocefin with a lower binding free energy, indicating tighter binding, compared with other antibiotics. Key residues involved

* Corresponding authors. Address: State Key Laboratory of Drug Research, Shanghai Institute of Materia Medica, Chinese Academy of Sciences, 555 Zuchongzhi Road, Shanghai 201203, China (C. Luo). Fax: +86 21 50807088.
E-mail addresses: heishh@fzu.edu.cn (Y. Chen), cluo@mail.shcnc.ac.cn (C. Luo).
[1] These authors contributed equally to this work.

0006-291X/$ - see front matter © 2013 Elsevier Inc. All rights reserved.
http://dx.doi.org/10.1016/j.bbrc.2012.12.141

in substrate binding were identified through energy decomposition analysis, and two mutant residues present only in NDM-1, namely, Ile35 and Lys216, were found to be responsible for tighter binding of NDM-1 to nitrocefin compared with its homologs IMP-1 and CcrA.

Loop L1, a conserved loop adjacent to the active site of B1 MBLs, was also found to be critical for both substrate recognition and enzyme activity. Dyson et al. [11] compared the dynamic properties of loop L1 between the inhibitor bound state and the apo state of CcrA and suggested that the broad substrate specificity and tight substrate binding of the CcrA enzyme could be attributed to the malleability of loop L1. Consistent with their study, Yang et al. [12] found that deletion of loop L1 in CcrA dramatically reduces both its hydrolytic activity and affinity for all β-lactams. Loop L1 in IMP-1 B1 MBLs was also found to be involved in substrate binding by molecular modeling and mutagenesis experiments [13]. However, the function of loop L1 in NDM-1 has not been thoroughly studied. In the present study, we explored the dynamic characteristics of loop L1 and its interactions with different substrate and found that loop L1 in NDM-1 may play an important role in substrate recognition and binding. Our study provides important insights into the structural basis for substrate binding and catalysis properties of NDM-1 and may have significant implications for the discovery of small molecules as effectors against NDM-1-induced antibiotic resistance.

2. Materials and methods

2.1. Molecular docking simulation

To obtain the starting structure of enzyme-substrate (ES) for simulation, molecular docking was performed with Maestro v9.0 (Schrodinger, Inc.) [14]. Ampicillin (penicillin), nitrocefin (cephalosporin), and meropenem (carbapenem), three common antibiotics from different β-lactam families, were first processed by the LigPrep [15] module to produce the corresponding low-energy three dimensional structures. Hydrogen atoms and protein charges were added during a brief relaxation period using the Protein Preparation Wizard module in Maestro to relieve steric clashes. Restrained partial minimization was terminated when the root-mean-square deviation (RMSD) reached a maximum value of 0.3 Å. The protein structure was derived from the NDM-1/ampicillin complex structure published in the Protein Data Bank (PDB). The grid-enclosing box was centered on the ligand in the crystal structure (PDB entry 3Q6X) [16] to enclose residues located within 15 Å. Each β-lactam antibiotic structure was then docked into the active site of NDM-1 with extra-precision (XP) docking to generate minimized poses and the Glide scoring function (G-Score) was used to select the final poses for each β-lactam antibiotic. Together with previously reported studies on the binding mode [17–19], three enzyme-substrate (ES) complex models were constructed.

2.2. MD simulation

MD simulations were performed on the three ES complexes obtained from molecular docking. Before simulations, the protonation states of ionizable residues were determined using the H++ program [20]. Each complex model was surrounded by a periodic box of transferable intermolecular potential 3P [21] water molecules that extend 12 Å from the protein atoms. Counter-ions were added to neutralize each simulation system. The parm99SB version of the all-atom assisted model building and energy refinement (AMBER) force field was used to represent the protein system. Atom charges of the three antibiotics were calculated using the restrained electrostatic potential method [22] encoded in the AMBER suite of programs [23] at the RHF/6-31G* level. Covalent and non-bonded parameters for the three antibiotic atoms were assigned by analogy or interpolation from those already present in the AMBER force field. The charges and force field parameters for the Zn-ligand center (two Zn ions, hydroxide, and six residues coordinated with Zn1 and Zn2) were calculated by the MCPB approach [24].

Before MD simulations, energy was minimized (8000 steps for the water molecules followed by 6000 steps for the whole system) for each solvated system to remove poor contacts between the solute and the solvent. All MD simulations were conducted using the SANDER program included in the AMBER package (version 10.0) at constant temperature and pressure and periodic boundary conditions with a time step of 2 fs. The SHAKE algorithm [25] was used to constrain all hydrogen atom bonds. Electrostatic interactions were calculated using the particle-mesh Ewald method [26]. The non-bonded cutoff was set to 10.0 Å, and the non-bonded pairs were updated every 25 steps. The temperature (300 K) and pressure (1 atm = 101.3 kPa) of the system were controlled during the MD simulations by applying the algorithm developed by Berendsen et al. [27]. The temperature and pressure coupling parameters were set to 1 ps.

2.3. Binding free energy calculation by MM-PBSA method

Based on the equilibrated dynamic trajectory, the binding free energy of each complex ES system was calculated using the MM-PBSA method encoded in the AMBER 10.0 program [23]. A total of 500 snapshots from the trajectory were extracted every 60 ps, and the MM-PBSA calculation was performed on each snapshot using the MMPBSA.PY module in AMBER 10.0.

2.4. Computational alanine-scanning mutagenesis

To further validate the contributions of key residues in the interaction with nitrocefin, computational alanine-scanning mutagenesis was performed on NDM-1-Nitrocefin complex, and the free energy of mutated NDM-1 binding with nitrocefin was calculated using the MM-PBSA method. The structures of the NDM-1-Nitrocefin complex were taken from the same snapshot of the complex trajectory. The alanine mutant structures were generated by altering the coordinates of the wild-type trajectory. This involved deleting atoms and truncating the mutated residue at C^{γ} by replacing with a hydrogen atom. A total of 500 snapshots were obtained for energy calculation. The relative binding free energy is the free energy difference between the wild-type and alanine mutants.

3. Results and discussion

3.1. Steady RMSDs values indicate that MD trajectories are reliable for post analysis

As shown in Fig. 1, all of the starting structures of the three complexes used in subsequent MD simulations share some similar features. The oxygen atom of the carbonyl group of -lactam ring orients toward Zn1 and that of the carboxylate group of the -lactam antibiotic is in a position where it can interact with Zn2 directly. To explore the dynamic traits of the different ES complexes, 30 ns MD simulations were performed on each ES complex model. To examine the structural stability of the ES complex during MD simulations, the time evolution of weighted RMSDs for backbone atoms of the NDM-1 protein and heavy atoms of the three β-lactam antibiotics from their initial positions ($t = 0$) were calculated. As illustrated in Figs. S2 and S3, RMSD values of the three ES complexes were found to be between 0.5 and 1.5 Å in all simulations. Steady RMSD values for the heavy atoms of

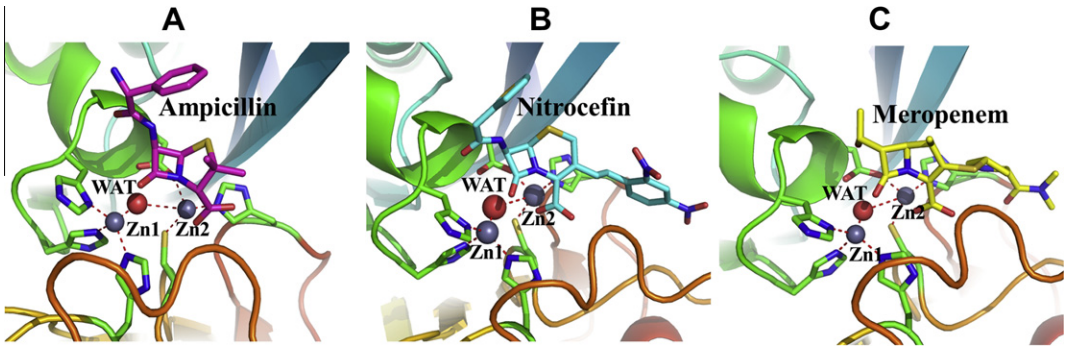

Fig. 1. The starting structures used for MD simulations obtained by molecular docking. (A) NDM-1-Ampicillin complex, (B) NDM-1-Nitrocefin complex, and (C) NDM-1-Meropenem complex.

the protein indicate well-equilibrated states of the systems and relatively stable catalytic cavity of each model during MD simulations. Steady RMSD values for the heavy atoms of -lactam antibiotics indicate that each antibiotic remained stable in the catalytic cavity. Both the steady RMSD values show the reliability of these MD trajectories and suggest the suitability for post analysis.

3.2. H-bond and hydrophobic interaction analyses revealed a well-defined substrate pocket for diverse substrates

To probe the molecular interactions between NDM-1 and the three β-lactam antibiotics, the H-bonds and hydrophobic interactions of the three complexes were analyzed based on MD trajectories (Tables 1 and 2). In the NDM-1-Ampicillin complex, a conserved H-bond between ND2 atom of the Asn220 residue and the oxygen atom (O1) of the carbonyl group of the β-lactam ring was revealed by the high H-bond occupancy rate (87.53%). In the NDM-1-Meropenem complex, two conserved H-bonds form between NDM-1 and the meropenem substrate. The NZ atom of Lys211 forms H-bonds with the O3 and O4 oxygen atoms of the carboxylate group of the β-lactam antibiotic, exhibiting occupancy rates of 92.2% and 61.06%, respectively, in the MD simulations. In the NDM-1-Nitrocefin complex, the ND2 atom of Asn220 makes H-bonds with the oxygen atom (O1) of the carbonyl group of the β-lactam ring, as revealed by an occupancy rate of 88.13%. The NZ atom of Lys211 forms relatively conserved H-bonds with the O3 and O4 oxygen atoms of the carboxylate group of the β-lactam ring of the nitrocefin substrate, exhibiting H-bond occupancy rates of 89.66% and 53.4%, respectively. The importance of the conserved residue Lys211 for substrate binding indicated by our simulation results is consistent with findings of previous mutagenesis studies [19].

NDM-1 has a relatively hydrophobic pocket. Thus, the non-polar contact between active site residues and small molecules cannot be ignored. We calculated the occupancy rate of hydrophobic interactions between active site residues and the three substrates based on MD trajectories (Table 2). Our results show slight differences among residues involved in hydrophobic interactions between NDM-1 and different substrates. Residues Leu65, Met67, and Phe70 in loop L1, Trp93, and Gln123 have more intense hydrophobic interactions with ampicillin and nitrocefin compared with meropenem, which may be caused by the larger hydrophobic groups in the acylamino side chain of ampicillin and nitrocefin. Such hydrophobic groups were not observed at the same position for meropenem. Taken together, our results indicate that extensive polar and non-polar interactions between NDM-1 and substrates provide suitable environment for catalytic reactions.

Table 1
Hydrogen bonds existing in the three ES complexes and their occupancies during the 30 ns MD simulation. Only H-bond occupancies >50% are shown.

Substrate	H-bond donor	H-bond acceptor	Occupancy rate (%)
Ampicillin	Asn220:ND2	AMP:O1	87.53
Nitrocefin	Lys211:NZ	NIT:O3	89.66
	Lys211:NZ	NIT:O4	53.40
	Asn220:ND2	NIT:O1	88.13
Meropenem	Lys211:NZ	MER:O3	92.20
	Lys211:NZ	MER:O4	61.06

Table 2
Residues involved in hydrophobic interactions with the substrate during the simulation time and the corresponding occupancy rate.

Substrate			
Residue	Ampicillin	Nitrocefin	Meropenem
Ile35	26%	90%	47%
Leu65	50%	9%	0%
Met67	83%	51%	5%
Phe70	47%	43%	17%
Val73	15%	33%	53%
Trp93	79%	31%	0%
His122	87%	19%	66%
Gln123	42%	16%	0%
Asp124	58%	25%	0%
His189	10%	51%	64%
Lys211	0%	25%	23%
Ser217	0%	14%	16%
Gly219	02%	84%	73%
Asn220	46%	87%	18%
His250	37%	90%	85%

3.3. Key residues involved in substrates binding were identified by energy decomposition

To further explore the molecular interactions between NDM-1 and the three β-lactam antibiotics, the binding free energy values of the three NDM-1/substrate complexes were calculated using the MM-PBSA method encoded in the AMBER 10 program. As shown in Table 3, NDM-1 shows the tightest binding to nitrocefin

Table 3
The binding free energy of NDM-1 to different substrates calculated by the MM-PBSA method and the experimental Km (μm) values. All calculated values are given in kcal/mol. ΔG = ΔGgas + ΔGsolv. ΔGgas represents the binding free energy in vacuum and ΔGsolv represents the solvation free energy change calculated by the MM-PBSA method.

Substrate	**ΔGgas**	**ΔGsolv**	**ΔG**	**Km (μm)**
Ampicillin	−139.57	122.08	−17.49	310 ± 30
Nitrocefin	−100.55	65.68	−35.41	1.3 ± 0.2
Meropenem	−106.68	82.67	−24.01	54 ± 3

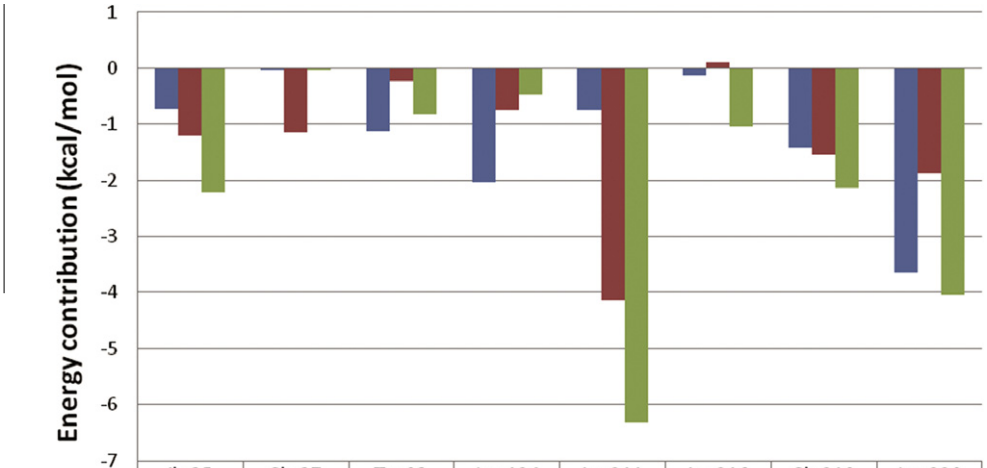

	Ile 35	Gln 37	Trp 93	Asp 124	Lys 211	Lys 216	Gly 219	Asn 220
Ampicillin	-0.724	-0.035	-1.116	-2.047	-0.742	-0.127	-1.42	-3.648
Meropenem	-1.2	-1.142	-0.222	-0.757	-4.145	0.115	-1.547	-1.876
Nitrocefin	-2.218	-0.031	-0.825	-0.475	-6.318	-1.053	-2.144	-4.039

Fig. 2. Decomposition of binding free energy ΔG into contributions from residues in the binding pocket. Only residues with contribution >−1 kcal/mol are shown. Values that are more negative indicate more contributions to substrate binding by the corresponding residues.

Table 4
Computational alanine scanning results for NDM-1 and nitrocefin interaction residues. All values are given in kcal/mol. ΔG1 represents the binding free energy before the mutation, ΔG2 represents the binding free energy after mutation, and ΔΔG is the relative influence of the mutation on the binding free energy.

Residues	ΔG1	ΔG2	ΔΔG
Ile35	−35.41	−32.34	3.07
His189	−35.41	−31.62	3.79
Lys211	−35.41	−21.25	14.16
Lys216	−35.41	−33.82	1.59
Asn220	−35.41	−31.33	4.08

among the three antibiotics, and the order of calculated binding free energy is consistent with previous experiments [28]. To identify the residues crucial for substrate binding, the binding free energy was further decomposed into contributions from residues in the binding pocket. As illustrated in Fig. 2, eight residues (Ile35, Gln37, Trp93, Asp124, Lys211, Lys216, Gly219, and Asn220) contribute the most to substrate binding. According to the crystal structures of NDM-1 and biochemical studies on homologous enzymes, two conserved residues (Lys211 and Asn220) play key roles in substrate binding. In the energy decomposition simulations, these two residues contribute the most after binding with NDM-1 and all three antibiotics, which further indicates the important roles of Lys211 and Asn220, and validates the results of our computational models. Other residues in the active pocket of NDM-1 may also contribute to substrate binding. However, when NDM-1 interacts with the three antibiotics, a different set of residues play major roles in substrate binding: residues Trp93, Asp124, Gly219, and Asn220 in ampicillin; residues His189, Lys211, Gly219, and Asn220 in meropenem; and residues Ile35, His189, Lys211, Lys216, Gly219, and Asn220 in nitrocefin. This finding may explain the substrate diversity of NDM-1, and the tight binding affinity displayed by nitrocefin may aid in inhibitor design.

Interestingly, based on our calculated results, among the six identified residues that contributed most to NDM-1 binding to nitrocefin, four residues (His189, Lys211, Gly219 and Asn220) were found to be highly conserved in the B1 MBLs family, such as IMP-1 and CcrA MBLs. However, two mutant residues (Ile35 and Lys216) are present only in NDM-1 (Fig. S4). As shown by experimental data from other studies, NDM-1 binds to nitrocefin with higher affinity compared with IMP-1 and CcrA [28–30]. The mutant residues Ile35 and Lys216 may be responsible for this extra binding ability between NDM-1 and nitrocefin. These results are further validated by our computational alanine scanning results (Table 4).

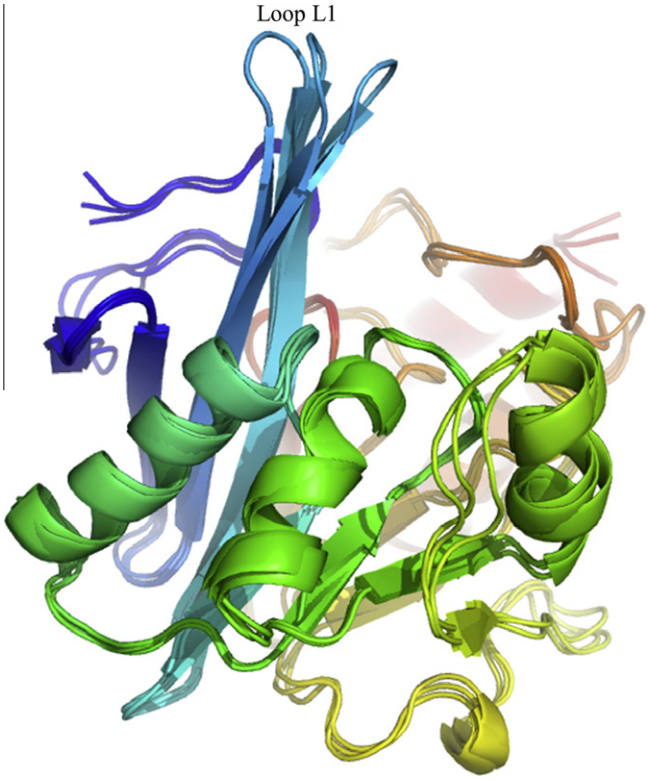

Fig. 3. Three distinct configurations of loop L1 obtained by clustering the MD trajectory of the apo-enzyme.

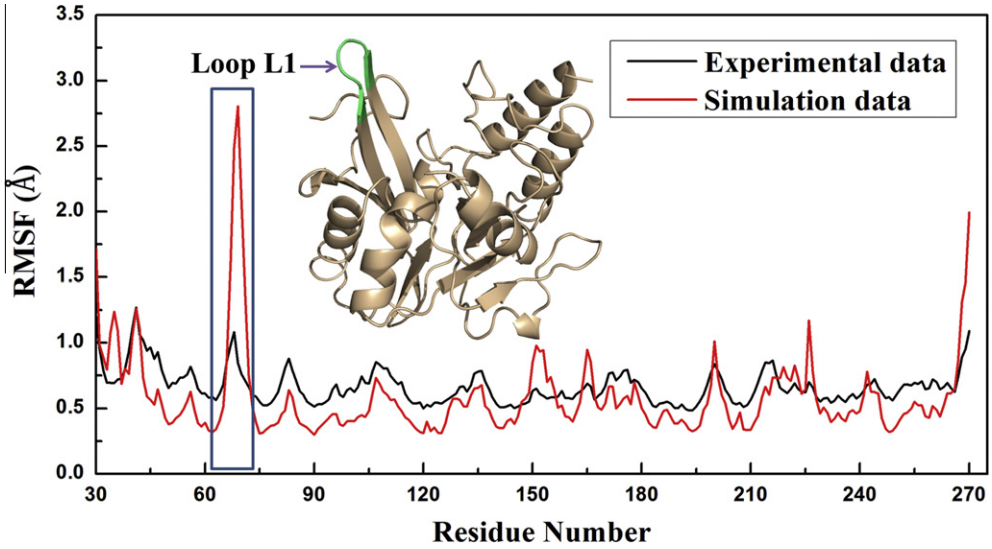

Fig. 4. Residue fluctuations obtained by average residual fluctuations over 30 ns simulations are shown in red, while experimental results calculated from B factors of NDM-1 (PDB code: 3Q6X) crystal structures are shown in black. (For interpretation of the references to color in this figure legend, the reader is referred to the web version of this article.)

3.4. The dynamic traits of loop L1 suggest its vital role in substrate recognition and binding

According to our results of MD simulation, the RMSD values for the backbone atoms of loop L1 (residues 65–73) and loop L2 (residues 205–225) are significantly higher than those of the whole enzyme (Fig. S5), indicating increased flexibility of loop L1 compared with that of other regions of NDM-1, which is consistent with experimental data reported in previous studies [31]. As illustrated in Fig. 3, when the conformations extracted from MD trajectories were clustered based on the RMSD values of loop L1, three distinct conformations of loop L1 were found. This finding is consistent with the root-mean-square fluctuation (RMSF) of the backbone atoms of NDM-1 calculated based on the apo-enzyme MD trajectory to the B-factors of NDM-1 crystal structure ($B = 8\pi^2 * RMSF^2/3$), which shows that the results of our simulation models could capture the main feature of the atomic movement of NDM-1 (Fig. 4). As expected, this region of loop L1 was found to have the largest RMSF value when no substrate was bound to the active site. However, when NDM-1 was bound to its substrates (NDM-1-Ampicillin, NDM-1-Nitrocefin, and NDM-1-Meropenem), the RMSF values of loop L1 decreased significantly (Fig. S6), which indicates that loop L1 could be stabilized by interactions with substrate molecules. By inspecting the stabilizing interactions between loop L1 and small substrate molecules, we found that the hydrophobic interactions were the major determinant in stabilization. Although their contributions to hydrophobic interactions are slightly different with different substrates, residues Leu65, Met67, Phe70, and Val73 in loop L1 are all involved in hydrophobic interactions (Table 2). These findings emphasize the role of loop L1 in substrate binding and recognition, and suggest a mutual stabilizing interaction between loop L1 and NDM-1 substrates.

Acknowledgments

This work was support by grants from National High Technology Research and Development Program of China (2012AA020302 and 2012AA020301), National Natural Science Foundation of China (21021063, 81230076, 21210003, and 21073034), the Key Project of Chinese National Programs for Fundamental Research and Development (2009CB918502), the Natural Science Foundation of the Fujian Province (2010J05023), the National Science and Technology Major Project "Key New Drug Creation and Manufacturing Program" (2013ZX09507-004). Computation resources were partially supported by Computer Network Information Center, Chinese Academy of Sciences and Shanghai Supercomputing Center.

Appendix A. Supplementary data

Supplementary data associated with this article can be found, in the online version, at http://dx.doi.org/10.1016/j.bbrc.2012.12.141.

References

[1] S.M. Drawz, R.A. Bonomo, Three decades of beta-lactamase inhibitors, Clin. Microbiol. Rev. 23 (2010) 160–201.
[2] J.F. Fisher, S.O. Meroueh, S. Mobashery, Bacterial resistance to beta-lactam antibiotics: compelling opportunism, compelling opportunity, Chem. Rev. (Washington, DC, U.S.) 105 (2005) 395–424.
[3] K. Bush, G.A. Jacoby, Updated functional classification of beta-lactamases, Antimicrob. Agents Chemother. 54 (2010) 969–976.
[4] M.W. Crowder, J. Spencer, A.J. Vila, Metallo-beta-lactamases: novel weaponry for antibiotic resistance in bacteria, Acc. Chem. Res. 39 (2006) 721–728.
[5] K. Bush, Alarming beta-lactamase-mediated resistance in multidrug-resistant Enterobacteriaceae, Curr. Opin. Microbiol. 13 (2010) 558–564.
[6] K.M. Papp-Wallace, A. Endimiani, M.A. Taracila, R.A. Bonomo, Carbapenems: past, present, and future, Antimicrob. Agents Chemother. 55 (2011) 4943–4960.
[7] F.J. Perez-Llarena, G. Bou, Beta-lactamase inhibitors: the story so far, Curr. Med. Chem. 16 (2009) 3740–3765.
[8] D. Yong, M.A. Toleman, C.G. Giske, H.S. Cho, K. Sundman, K. Lee, T.R. Walsh, Characterization of a new metallo-beta-lactamase gene, bla (NDM-1), and a novel erythromycin esterase gene carried on a unique genetic structure in klebsiella pneumoniae sequence type 14 from India, Antimicrob. Agents Chemother. 53 (2009) 5046–5054.
[9] J.M. Rolain, P. Parola, G. Cornaglia, New Delhi metallo-beta-lactamase (NDM-1): towards a new pandemia?, Eur J. Clin. Microbiol. Infect. Dis. 16 (2010) 1699–1701.
[10] P. Nordmann, L. Dortet, L. Poirel, Carbapenem resistance in Enterobacteriaceae: here is the storm!, Trends Mol Med. 18 (2012) 263–272.
[11] J.J. Huntley, S.D. Scrofani, M.J. Osborne, P.E. Wright, H.J. Dyson, Dynamics of the metallo-beta-lactamase from *Bacteroides fragilis* in the presence and absence of a tight-binding inhibitor, Biochemistry 39 (2000) 13356–13364.
[12] Y. Yang, D. Keeney, X. Tang, N. Canfield, B.A. Rasmussen, Kinetic properties and metal content of the metallo-beta-lactamase CcrA harboring selective amino acid substitutions, J. Biol. Chem. 274 (1999) 15706–15711.
[13] C. Moali, C. Anne, J. Lamotte-Brasseur, S. Groslambert, B. Devreese, J. Van Beeumen, M. Galleni, J.M. Frere, Analysis of the importance of the metallo-

beta-lactamase active site loop in substrate binding and catalysis, Chem. Biol. 10 (2003) 319–329.
[14] R.A. Friesner, J.L. Banks, R.B. Murphy, T.A. Halgren, J.J. Klicic, D.T. Mainz, M.P. Repasky, E.H. Knoll, M. Shelley, J.K. Perry, D.E. Shaw, P. Francis, P.S. Shenkin, Glide: a new approach for rapid, accurate docking and scoring. 1. Method and assessment of docking accuracy, J. Med. Chem. 47 (2004) 1739–1749.
[15] LigPrep, version 2.5: Schrödinger, LLC., New York, NY, 2011.
[16] H. Zhang, Q. Hao, Crystal structure of NDM-1 reveals a common beta-lactam hydrolysis mechanism, FASEB J. 25 (2011) 2574–2582.
[17] Z. Wang, W. Fast, A.M. Valentine, S.J. Benkovic, Metallo-beta-lactamase: structure and mechanism, Curr. Opin. Chem. Biol. 3 (1999) 614–622.
[18] S. Bounaga, A.P. Laws, M. Galleni, M.I. Page, The mechanism of catalysis and the inhibition of the *Bacillus cereus* zinc-dependent beta-lactamase, Biochem. J. 331 (Pt 3) (1998) 703–711.
[19] Z. Liang, L. Li, Y. Wang, L. Chen, X. Kong, Y. Hong, L. Lan, M. Zheng, C. Guang-Yang, H. Liu, X. Shen, C. Luo, K.K. Li, K. Chen, H. Jiang, Molecular basis of NDM-1, a new antibiotic resistance determinant, PLoS One 6 (2011) e23606.
[20] J.C. Gordon, J.B. Myers, T. Folta, V. Shoja, L.S. Heath, A. Onufriev, H++: a server for estimating pKas and adding missing hydrogens to macromolecules, Nucleic Acids Res. 33 (2005) W368–371.
[21] W.L. Jorgensen, J. Chandrasekhar, J.D. Madura, R.W. Impey, M.L. Klein, Comparison of simple potential functions for simulating liquid water, J. Chem. Phys. 79 (1983) 926–935.
[22] C.I. Bayly, P. Cieplak, W.D. Cornell, P.A. Kollman, A well-behaved electrostatic potential based method using charge restraints for deriving atomic charges – the resp model, J. Phys. Chem. 97 (1993) 10269–10280.
[23] D.A. Case, T.E. Cheatham, T. Darden, H. Gohlke, R. Luo, K.M. Merz, A. Onufriev, C. Simmerling, B. Wang, R.J. Woods, The Amber biomolecular simulation programs, J. Comput. Chem. 26 (2005) 1668–1688.
[24] M.B. Peters, Y. Yang, B. Wang, L. Fusti-Molnar, M.N. Weaver, K.M. Merz, Structural survey of zinc-containing proteins and development of the zinc AMBER force field (ZAFF), J. Chem. Theory Comput. 6 (2010) 2935–2947.
[25] J.P. Ryckaert, G. Ciccotti, H.J.C. Berendsen, Numerical-integration of cartesian equations of motion of a system with constraints – molecular-dynamics of n-alkanes, J. Comput. Phys. 23 (1977) 327–341.
[26] T. Darden, D. York, L. Pedersen, Particle mesh Ewald – an N. Log(N) method for Ewald sums in large systems, J. Chem. Phys. 98 (1993) 10089–10092.
[27] H.J.C. Berendsen, J.P.M. Postma, W.F. Vangunsteren, A. Dinola, J.R. Haak, Molecular-dynamics with coupling to an external bath, J. Chem. Phys. 81 (1984) 3684–3690.
[28] P.W. Thomas, M. Zheng, S. Wu, H. Guo, D. Liu, D. Xu, W. Fast, Characterization of purified New Delhi metallo-beta-lactamase-1, Biochemistry 50 (2011) 10102–10113.
[29] Y. Yamaguchi, T. Kuroki, H. Yasuzawa, T. Higashi, W. Jin, A. Kawanami, Y. Yamagata, Y. Arakawa, M. Goto, H. Kurosaki, Probing the role of Asp-120(81) of metallo-beta-lactamase (IMP-1) by site-directed mutagenesis, kinetic studies, and X-ray crystallography, J. Biol. Chem. 280 (2005) 20824–20832.
[30] M.P. Yanchak, R.A. Taylor, M.W. Crowder, Mutational analysis of metallo-beta-lactamase CcrA from *Bacteroides fragilis*, Biochemistry 39 (2000) 11330–11339.
[31] V.L. Green, A. Verma, R.J. Owens, S.E. Phillips, S.B. Carr, Structure of New Delhi metallo-beta-lactamase 1 (NDM-1), Acta Crystallogr. Sect. F Struct. Biol. Cryst. Commun. 67 (2011) 1160–1164.